



Molecular process of glucose uptake and glycogen storage due to hamamelitannin via insulin signalling cascade in glucose metabolism

Praveen Kumar Issac¹ · Ajay Guru¹ · Sri Sneha Chandrakumar² · Christy Lite³ · N. T. Saraswathi⁴ · Mariadhas Valan Arasu⁵ · Naif Abdullah Al-Dhabi⁵ · Aziz Arshad^{6,7} · Jesu Arockiaraj¹

Received: 3 June 2020 / Accepted: 10 August 2020 / Published online: 18 August 2020
© Springer Nature B.V. 2020

Abstract

Understanding the mechanism by which the exogenous biomolecule modulates the GLUT-4 signalling cascade along with the information on glucose metabolism is essential for finding solutions to increasing cases of diabetes and metabolic disease. This study aimed at investigating the effect of hamamelitannin on glycogen synthesis in an insulin resistance model using L6 myotubes. Glucose uptake was determined using 2-deoxy-D-[1-³H] glucose and glycogen synthesis were also estimated in L6 myotubes. The expression levels of key genes and proteins involved in the insulin-signaling pathway were determined using real-time PCR and western blot techniques. The cells treated with various concentrations of hamamelitannin (20 μM to 100 μM) for 24 h showed that, the exposure of hamamelitannin was not cytotoxic to L6 myotubes. Further the 2-deoxy-D-[1-³H] glucose uptake assay was carried out in the presence of wortmannin and Genistein inhibitor for studying the GLUT-4 dependent cell surface recruitment. Hamamelitannin exhibited anti-diabetic activity by displaying a significant increase in glucose uptake (125.1%) and glycogen storage (8.7 mM) in a dose-dependent manner. The optimum concentration evincing maximum activity was found to be 100 μm. In addition, the expression of key genes and proteins involved in the insulin signaling pathway was studied to be upregulated by hamamelitannin treatment. Western blot analysis confirmed the translocation of GLUT-4 protein from an intracellular pool to the plasma membrane. Therefore, it can be conceived that hamamelitannin exhibited an insulinomimetic effect by enhancing the glucose uptake and its further conversion into glycogen by regulating glucose metabolism.

Keywords Hamamelitannin · Insulin signalling · Molecular process · Glycogen synthesis · Type II diabetes mellitus

Abbreviations

DM	Diabetes mellitus	PBS	Phosphate buffer saline
T2DM	Type 2 diabetic mellitus	DMSO	dimethylsulfoxide
IRS	insulin receptor substrate	KRPH	Krebs–Ringer phosphate buffer solution
PI3Ks	phosphoinositide 3-kinases	IRTK	Insulin receptor tyrosine kinase
GLUT-4	glucose transporter type 4	DEPC	Diethyl pyrocarbonate
GS	Glycogen synthase	IRβ	Insulin receptor β
ROS	Reactive oxygen species	GSK-3β	Glycogen synthase kinase 3β
DMEM	Dulbecco's modified eagle's medium		
NCCS	National Center for Cell Science		

Electronic supplementary material The online version of this article (<https://doi.org/10.1007/s11033-020-05728-5>) contains supplementary material, which is available to authorized users.

✉ Jesu Arockiaraj
jesuaraj@hotmail.com

Extended author information available on the last page of the article

Introduction

Diabetes mellitus (DM) is a metabolic disorder with the clinical manifestation of long-lasting hyperglycaemia. It has a profound influence on protein, fat and carbohydrate metabolism, causing inappropriate insulin release, activity or a combination of both. Its long-term impact result in deterioration and affect the function of organs. As DM progresses in severe state, leads to ketoacidosis or a non ketotic

hyperosmolar state which may further lead to brain damage and even proved to be fatal without a timely treatment. In the long run, DM could also result in visual impairment, renal disorder, diabetic foot ulcers and infertility. In addition to these morbidities, the patient is also prone to peripheral vascular, cardiovascular and cerebrovascular disorders [1–3].

Type 2 diabetic mellitus (T2DM) condition result from factors involving lack of insulin sensitivity exhibited by the liver and skeletal muscle cells, it also affects the other physiological end-points such as *de novo* synthesis of glucose in liver and altered levels of free fatty acids derived from the breakdown of triglycerides from adipose tissue, even though the blood glucose levels can be achieved through diet restrictions and physical activity to an extent. In severe cases, oral drugs and/or insulin administration is required for T2DM treatment [4–6].

In accordance with the metabolic functioning of the tissue and organs, the effect of insulin, its deficiency and resistance are varied. In particular, muscle and fat cells depend on insulin for glucose transport [7]. Metabolism in the fasting state is primarily regulated by glucagon that induces glycogen breakdown, gluconeogenesis and ketone synthesis. The balance of insulin versus glucagon determines the level of activation or deactivation of the relevant enzymes [8]. Catecholamine regulates lipid and glycogen catabolism; glucocorticoids promotes gluconeogenesis, and lipid breakdown. Increased production of such hormones may also augment insulin sensitivity [8]. T2DM can be also manifested at the molecular level, such as dysregulation in insulin signalling mechanism as result of genetic polymorphisms in insulin receptor, insulin receptor substrate (IRS) proteins or phosphoinositide 3-kinases (PI3Ks). Aberrant glucose transporter type 4 (GLUT-4) function also suggested to be a contributory factor in the T2DM pathology [9]. Thus, T2DM is multifactorial disease resulting from the interaction of various altered physiological and cellular process together leading to disrupted glucose homeostasis.

The intracellular intake of glucose in muscle cells is primarily a insulin-dependent mechanism [10]. In post-prandial state insulin stimulates glycogen synthesis through the activation of glycogen synthase (GS). In basal state, myocytes do not only depend on glucose or glycogen for energy requirement. When low insulin levels are encountered, the condition stimulate the release of amino acids for gluconeogenesis during starvation, thus the protein synthesis is nearly reduced to half of its volume [11]. Muscle glycogenesis is decreased in the case of insulin resistance, which mainly results in reduced glucose levels inside the cells [12].

Hamamelis virginiana is a species of flowering shrub which contain a specific type of tannins referred as hamamelitannin (2'5-di-O-galloyl hamamelose). It is made up of two gallate moieties and one sugar units forming its molecular structure (E-Suppl Fig. 1). Hamamelitannin has

been studied to protect cells against ultraviolet B radiation-induced cell death, mainly mediated by the mechanism involved in scavenging of reactive oxygen species (ROS). The free radicals e.g. superoxide anion and hydroxy radicals are scavenging to act as an anti-aging agent in the skin [13, 14]. Hamamelitannin was also studied to show antibacterial activity against pathogenic organisms such as *Staphylococcus epidermidis*, *S. aureus*, *Acinetobacter baumannii* and *Candida albicans* [15]. Hamamelitannin exposure was shown selectively toxic against colon cancer cells [16]. Hamamelitannin treatment increased host survival following infection by inhibiting the bacterial biofilm formation [17]. Even though Hamamelitannin or *H. virginiana* extracts have been studied for their beneficial effects such as antioxidant, anti-aging and anti-bacterial characters, till now there are no reports characterizing their antidiabetic or insulinomimetic activity related to glucose metabolism. In this study, we have reported the effect of hamamelitannin on glycogen synthesis in an insulin resistance model using L6 myotubes.

Materials and methods

Chemicals and reagents

Hamamelitannin was obtained from Sigma-Aldrich, India (purity $\geq 98.0\%$). The reagents and chemicals such as MTT, acrylamide, bisacrylamide, SDS, APS, sucrose, sodium azide, TEMED, Tris HCl, Tris BASE, Glycine, β -mercapto ethanol, bovine serum albumin, HEPES, PMSF, Aprotinin, Pepstatin, EGTA, Insulin, Rosiglitazone, Trypsin EDTA, DMSO, Phosphate buffer saline (10 \times) and Dulbecco's modified eagle's medium (DMEM) (4.5 g glucose, 4.0 mM L-glutamine, 1 mM sodium pyruvate and 1.5 g/L of sodium bicarbonate) were of higher analytical grade and purchased from Himedia, Mumbai, India. FBS was acquired from GIBCO Life Technologies, USA. Wortmannin and genistein were procured from Calbiochem, Germany. TRIZOL reagent was obtained from Sigma-Aldrich, USA. Quantitative PCR analysis was carried out using KAPA SYBR[®] FAST qPCR Master Mix (2 \times) reagents and primers were obtained from EUROFINS. Antibodies including anti-GLUT-4, p-Insulin R β antibody, Anti-GSK3 pAb (serine phosphorylation 9th residue) were obtained from Calbiochem, Germany. Secondary antibody conjugated with HRP and anti-goat IgG-FITC were obtained from Santa Cruz Biotechnologies, USA. Luminol reagent was obtained from Santa Cruz, USA. All the other chemicals and reagents used unless otherwise stated were of high analytical grade.

In vitro assays for anti-diabetic activity of hamamelitannin

Maintenance of L6 myoblast cell line

L6 myoblast was procured from National Center for Cell Science (NCCS) Pune, India. The cells were obtained at passage number 14. The obtained cells were cultured in DMEM medium with 10% FBS supplemented with antibiotic-antimycotic solution and incubated in laboratory condition at 37 °C in 5% CO₂. The cells passaged and cryopreserved in liquid nitrogen for further experiments.

Differentiation of L6 myoblasts into L6 myotubes for in vitro assessment

L6 myoblast was maintained in Dulbecco's Modified Eagle Medium (DMEM) with high glucose (25 mmol/L) supplemented with 10% fetal bovine serum (FBS) and with a cocktail containing antibiotic-antimycotic solution (10,000 U Penicillin), 10 mg Streptomycin and 25 µg Amphotericin B per mL in 0.9% normal saline. Cells were maintained in 5% CO₂ environment at 37 °C [18]. For differentiation, 2 days of post-confluence, the L6 myoblasts cells were transferred to DMEM containing 2% FBS. The cell differentiation was confirmed through the development of cell multinucleation. The differentiated L6 myoblasts cells were further maintained in high glucose DMEM (25 mmol/L) medium for 24 h and used for the in vitro assessment [19].

Assessment of cell viability by MTT assay

Using MTT assay, the cell viability of L6 myoblasts cells were assessed [20]. Briefly, 3 × 10⁵ cells/wells, were seeded in a 96 well plate. The cells were treated with various concentrations of hamamelitannin (20, 40, 60, 80 and 100 µM) for 24 h. Triton X-100 (0.01%) served as the positive control. The cells were washed with 1X Phosphate buffer saline (PBS). Twenty µL of MTT reagent (5 mg/mL) was added to wells and incubated in dark condition for 4 h. Later the supernatant was aspirated, 100 µL of dimethylsulfoxide (DMSO) was added to all the wells and absorbance was measured at 570 nm using ELISA plate reader (Multiskan GO, Thermo scientific, Finland). The percentage of cell viability was determined by using the following calculation:

$$\% \text{Cell viability} = \frac{\text{OD of treated sample}}{\text{OD of control}} \times 100$$

Glucose uptake assay

The 2-deoxy-D-[1-³H] glucose uptake was performed in L6 myoblasts as previously described [21]. Briefly, 0.75 × 10⁶ L6 myotubes were cultured in a 24 well plate and differentiated for two days as described elsewhere. After serum deprivation for 8 h, the cells were treated with various concentrations of hamamelitannin (20, 40, 60, 80 and 100 µM). The cells were treated with 10 nM of insulin for 20 min prior to the assay. 10 nM insulin maintains a base level glucose uptake by the cells. The 10 nM of insulin was used in the current study because, as this concentration is within the physiological range [22]. 100 nM of insulin was used as positive control. Following incubation, the cells were washed with 1 mL of HEPES buffer and Krebs–Ringer phosphate buffer solution (KRPH). Followed by an incubation along with 0.5 µCi of 2-deoxy-D-[1-³H] glucose for 20 min. The process was stopped by removing the KRPH solution containing 2-deoxy-D-[1-³H] glucose and washed twice with ice-cold HEPES-buffer. Cell lysis was performed with 0.1% SDS and following the lysates were transferred to a 96 well plate to assess the cell-associated radioactivity using a liquid scintillation counter. The non-specific uptake of glucose was corrected using 10 µM of cytochalasin B (5–10% of total uptake). Assays were conducted in triplicates for concordance. Extent of radioactivity from 2-deoxy-D-[1-³H] glucose incorporated cells was quantified in a scintillation counter and the results were compared with respect to untreated control.

Glucose uptake in L6 myotubes in presence of IRTK and PI3K inhibitors

2-Deoxy-D-[1-³H]-glucose uptake was performed with insulin receptor tyrosine kinase (IRTK) and PI3K inhibitors (genistein and wortmannin) as described [23]. Briefly, L6 myotubes were subjected to serum starvation for 8 h, then followed by the treatment with 50 nM of genistein and 100 nM of wortmannin for 30 min. After treating the cells with any one of the inhibitors either genistein or wortmannin, the cells were again treated with 100 µM of hamamelitannin for 24 h and 2-deoxy-D-[1-³H]-glucose uptake assay was performed as mentioned earlier and the results were compared with respective inhibitor untreated group.

Estimation of glycogen content in L6 myotubes

L6 myotubes were serum starved for 8 h accompanied by incubation with hamamelitannin (20 to 100 µM) 10 nM insulin, thus the reaction stimulated. 100 nM of insulin was used as positive control. The cells were incubated with 10 mM of glucose dissolved in HEPES (4-(2-hydroxyethyl)-1-piperazineethanesulfonic acid) buffer for 30 min. Later,

30% potassium hydroxide was added on to the wells and incubated for 5 min. The lysates were heated for 30 min at 70 °C followed by the addition of ice-cold ethanol (95%) and incubated overnight at 8 °C to enable glycogen precipitation. The pellet was obtained after centrifugation at 8000×g for 10 min. The pellet was dissolved in distilled water followed by the addition of anthrone reagent and cooled on ice for 10 min. This solution was heated at 80 °C for 10 min and again cooled using ice water. To estimate the glycogen content, the solution's absorbance was measured at 620 nm and glycogen was used as standard [24].

Isolation of RNA from L6 myotubes by TRIZOL method

L6 myotubes treated with 100 µM hamamelitannin was used for the total RNA isolation. The RNA extraction was carried out using trizol reagent. Briefly, after 24 h incubation, the cells were stimulated with 10 nM of insulin and incubated for 20 min. After the incubation, medium was removed from the plate and the cells were rinsed with 1 mL of 1× PBS. The cell lysate was obtained by adding 1 mL of TRIZOL solution and vigorously pipetted to lyse the cells. The cell lysate was transferred to 2 mL Eppendorf tube and inverted for 5–10 times and incubated in ice for 10 min. To this mixture, 200 µL of chloroform was added and inverted briefly for 4 to 5 times and incubated in ice for 10 min to facilitate precipitation, further centrifuged at 14,000 rpm for 20 min at 4 °C for phase-separation. The upper aqueous phase was transferred to the fresh vial and remaining solution was discarded and 500 µL of isopropanol was added and inverted 2 to 5 times and kept in ice for 10 min and centrifuged at 14,000 rpm for 10 min at 4 °C. The supernatant was discarded completely and the pellet was then air dried. The pellet was suspended

in Diethyl pyrocarbonate (DEPC) treated water and stored at – 20 °C and used within a day for further experiments [25].

Reverse transcription and Real time PCR analysis

RNA was isolated from the myotubes after the exposure period, converted to cDNA by reverse transcription [26–28] using MuLV reverse transcriptase enzyme (40 U/µL) [29–32]. The cDNA was further used for real-time PCR analysis carried out using KAPA SYBR FAST qPCR Master Mix [33–35] amplified with specific primers (Table 1). The $\Delta\Delta\text{ct}$ value was calculated after normalizing with GAPDH and the fold change was estimated using $2^{-\Delta\Delta\text{ct}}$ method.

Measurement of IRβ and GSK-3β by western blot analysis

L6 myoblasts were seeded in 6 well plates (5×10^5 cells/well) and induce to differentiate into L6 myotubes for two days. The L6 myotubes cells were dosed with 100 µM hamamelitannin for 24 h and stimulated with 10 nM of insulin for 15 min. After incubation, cells were rinsed with ice-cold 1X PBS and lysed with 1 mL of lysis buffer containing, HEPES 50 mM, NaCl 150 mM, EDTA 10 mM, $\text{Na}_4\text{P}_2\text{O}_7$ 10 mM, Sodium orthovanate 1 mM, NaF 50 mM, Aprotinin 10 µg/mL, Leupeptin 10 µg/mL and Triton X 100 [41]. Cell lysates were homogenized using a dounce homogenizer (20 strokes, 0.5 cycles, 10 pulses); 2 min each and lag time of 1 min for each pulse. Further, the cell homogenate was centrifuged at 12,000 rpm for 20 min at 4 °C to isolate total proteins. The protein concentration was determined using Bradford's method and proteins were separated using SDS-PAGE (5% stacking gel and 12% separating gel) and separated proteins were blotted on to nitrocellulose membrane. Then the membrane immunoblotted with the respective Insulin

Table 1 Primer sequences used for the amplification of genes studied

S.no.	Gene	Primer sequence	References
1	IRTK	Forward: 5' ATC TGG ATC CCC CTG ATA ACT GTC 3' Reverse: 5' ATG TGG GTG TAG GGG ATG TGT TCA 3'	GenBank ID: NM_017071
2	IRS-1	Forward: 5' AAG TGG CGG CAC AAG TCG AG 3' Reverse: 5' CGG GTG TAG AGA GCC ACC AG 3'	GenBank ID: XM_002749924
3	PI3K	Forward: 5' TGA CGC TTT CAA ACG CTA TC 3' Reverse: 5' CAG AGA GTA CTC TTG CAT TC 3'	[36]
4	GLUT-4	Forward: 5' CGG GAC GTG GAG CTG GCC GAG GAG 3' Reverse: 5' CCC CCT CAG CAG CGA GTG A 3'	[37]
5	GSK-3β	Forward: 5' GGT GAA TCG AGA AGA GCC AT 3' Reverse: 5' CTC CTG AGT CAC AAA GTT TG 3'	[38]
6	GS	Forward: 5' CGT GGT GAG AGG AAG GAA CTG AGC 3' Reverse: 5' CCG TCA GAC CGT GGA GAC A 3'	[39]
7	GAPDH	Forward: 5' CCA CCC ATG GCA AAT TCC ATG GCA 3' Reverse: 5' TCT AGA CGG CAG GTC AGG TCC ACC 3'	[40]

receptor β (IR β), Glycogen synthase kinase 3 β (GSK-3 β) and GLUT-4 antibodies. The immunosignals were detected using luminol/H₂O₂ reagent and visualized using chemiDoc XRS + imaging system (Biorad, USA). Protein quantification was done using densitometric scanning using Image Studio Lite version 5.2.

Sub cellular fractionation and western blot analysis for GLUT 4 translocation

Plasma membrane (PM) fraction was separated by density gradient centrifugation method using Sucrose (Sucrose 250 mmol/L, NaN₃ 5 mM, HEPES 20 mM, PMSF 200 μ M/L, Pepstatin 1 μ M/L, Aprotinin 1 μ M/L, EGTA 2 μ M/L, pH 7.4) [21]. Briefly, L6 myotubes (5×10^5 cells/well) after treatment with hamamelitannin (100 μ M) for 24 h were washed with 1 \times PBS and resuspended in buffer. Cell lysates was obtained using dounce homogenizer. The cell homogenate was centrifuged at $750 \times g$ for 5 min at 4 $^{\circ}$ C. The supernatant was centrifuged at $30,000 \times g$ for 40 min at 4 $^{\circ}$ C. The resultant pellet was re-suspended with buffer to constitute the PM fraction. The PM fraction was subjected to electrophoresis on 10% SDS-PAGE and transferred to nitrocellulose membrane. Then the membrane was blocked overnight with 5% skimmed milk at 4 $^{\circ}$ C and later immunoblotted with anti-GLUT 4 antibody.

Immunofluorescence analysis

For performing the immunofluorescence analysis, L6 myotubes were grown on coverslips and treated with the optimal concentration of the hamamelitannin (100 μ M) for 24 h. Formaldehyde (3.7%) dissolved in PBS is used for fixing the cells. The cell permeabilization was performed with PBS containing 0.01% Triton-X-100, for 10 min. The cells were blocked with 3% FBS in PBS for 10 min and then incubated with anti-goat GLUT-4 antibody (1:250 dilution) along with 3% FBS dissolved in PBS for 1 h at 4 $^{\circ}$ C. This was followed by incubation with anti-goat IgG-FITC (Santa Cruz Biotechnology, USA) used in 1:100 dilution. All the coverslips were washed thrice with PBS during each incubation step and mounted with Mowiol and used for imaging using confocal microscopy (Carl Zeiss laser scanning microscope LSM700, Austria). The excitation and emission levels were set at 468 nm and 543 nm, respectively [33].

Statistical analysis

All in vitro experiments were carried out in triplicates and the data were expressed as mean \pm SD of three independent experiments. The difference between mean values were analyzed using one-way ANOVA followed by Tukey's post hoc test for finding the statistical significance (level set at

$p < 0.05$). The data was analysed using Graph pad prism 5.03 statistical software (Graphpad software Inc. La Jolla, CA).

Results

Hamamelitannin on cell viability

Treatment of the cells with various concentrations of hamamelitannin (20 to 100 μ M) did not defect the cell viability, indicating that they were not cytotoxic to L6 myotube cells in the concentration tested (Fig. 1).

Hamamelitannin on glucose uptake by L6 cells

L6 myotubes were treated with various concentrations of hamamelitannin (20 to 100 μ M) to evaluate the glucose uptake activity. A dose-dependant increase in glucose uptake was observed in hamamelitannin exposure groups. The highest concentration (100 μ M) showed significantly ($p < 0.05$) enhanced ($125.1 \pm 2.5\%$ 2-deoxy-D-[1-³H]-glucose) uptake compared to the control, which enabled the uptake in L6 myotubes (Fig. 2).

IRTK and PI3K dependent 2-deoxy-D-[1-³H]-glucose uptake

Decrease in glucose uptake ($94.4 \pm 3.6\%$) was witnessed in the cells exposed with insulin pretreated with genistein, IRTK inhibitor. The presence of genistein significantly ($p < 0.05$) lowered the glucose uptake percentage, whereas the cells treated with the hamamelitannin (100 μ M) without inhibitor showed high glucose uptake ($213.9 \pm 2.5\%$). This

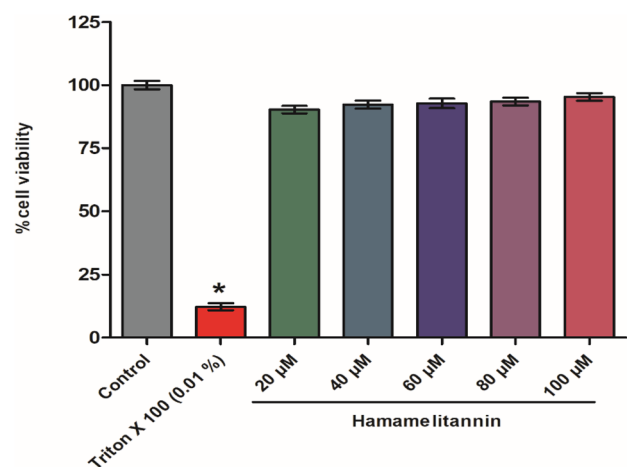


Fig. 1 Assessment of cell viability in the presence of hamamelitannin (20 μ M to 100 μ M) in L6 myoblasts. 0.01% Triton X-100 used as a positive control. Data shown depict the mean \pm S.D in triplicates of three independent experiments. * $p < 0.01$ as compared with control

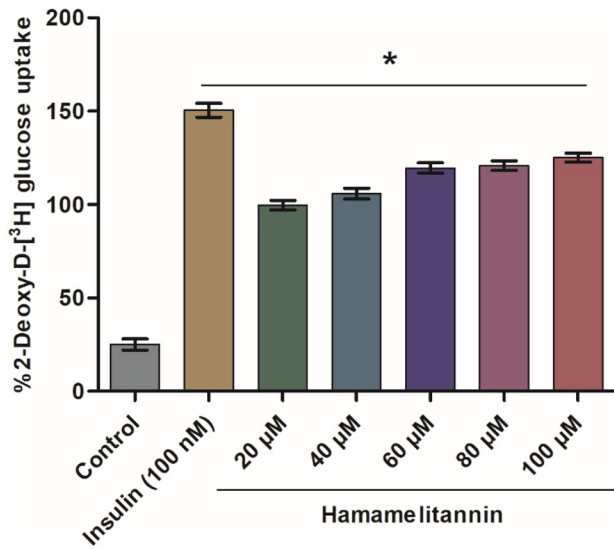


Fig. 2 Dose-response analysis of hamamelitannin on 2-deoxy-D-[1-³H]-glucose uptake in L6 myotubes for 24 h. The results were expressed as percentage (%) glucose uptake and were compared with respect to untreated control. 100 nM Insulin were used as positive controls. Data were expressed as mean \pm SD of three independent experiments. * $p < 0.05$ as compared with control

characterizes that hamamelitannin mediate glucose uptake activity through IRTK dependent mechanism (Fig. 3a).

The hamamelitannin upon pre-treatment with wortmannin exhibited a significant ($p < 0.05$) decrease in glucose uptake $96.7 \pm 2.1\%$ compared with the respective hamamelitannin (100 μ M) without inhibitor which showed $200.2 \pm 2.6\%$. Decrease ($84.4 \pm 2.6\%$) in glucose uptake activity was observed in group with insulin treatment (Fig. 3b).

Hamamelitannin on glycogen storage in L6 myotubes

The glycogen content in the cells treated with the hamamelitannin (20 to 100 μ M) and insulin were found to be significantly ($p < 0.05$) higher when compared to the control. The highest concentration of hamamelitannin (100 μ M) was found to increase (8.7 mM) the synthesis of glycogen in L6 myotubes (Fig. 4).

Hamamelitannin on expression of genes involved in insulin signaling cascades

To evaluate the impact of hamamelitannin on glucose signalling cascade the key genes such as IRTK, IRS-1, PI3K, GLUT-4, GSK-3 β and GS mRNA expression was quantified using Real Time-PCR. The results showed that hamamelitannin treated cells showed significant upregulation in the expression of genes: IRTK (2.8 fold), IRS-1 (2.7 fold) PI3K (2.9 fold), GSK-3 β (2.7 fold), GS (2.5 fold) and GLUT 4 (2.8

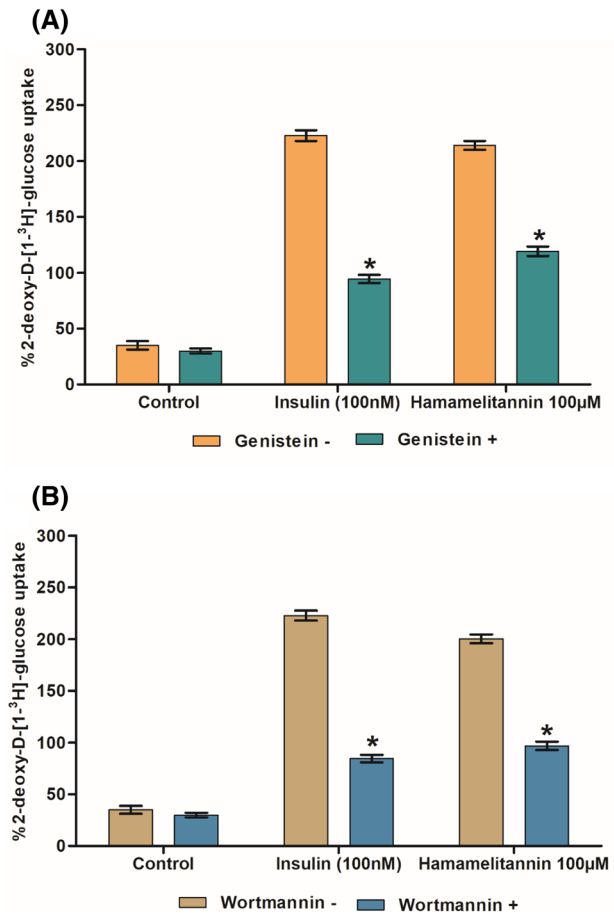


Fig. 3 2-Deoxy-D-[1-³H]-glucose uptake pattern of hamamelitannin 100 nM in the presence of IRTK inhibitor—genistein (a) and PI3K inhibitor—Wortmannin (b). 50 μ M Genistein and 100 μ M wortmannin were added to L6 myotubes 30 min prior to the incubation with 100 nM hamamelitannin, followed by 2-deoxy-D-[1-³H]-glucose uptake assay. 100 nM Insulin were used as positive controls. The results were expressed as % glucose uptake and were compared with the respective group. Data were expressed as mean \pm SD of three independent experiments. * $p < 0.05$ as compared with control

fold) when normalized and compared to the house keeping gene (Fig. 5a–f).

Hamamelitannin activated IR β and GSK-3 β in L6 myotubes

Western blot analysis revealed that L6 myotubes treated with highest concentration of hamamelitannin (100 μ M) significantly ($p < 0.05$) enhanced the phosphorylation of key insulin signaling marker IR β , similar to positive control as shown in (Fig. 6a). A 100 μ M hamamelitannin exposure group also showed a significant ($p < 0.05$) increase in phosphorylated GSK-3 β expression in the L6 myotubes (Fig. 6b and c).

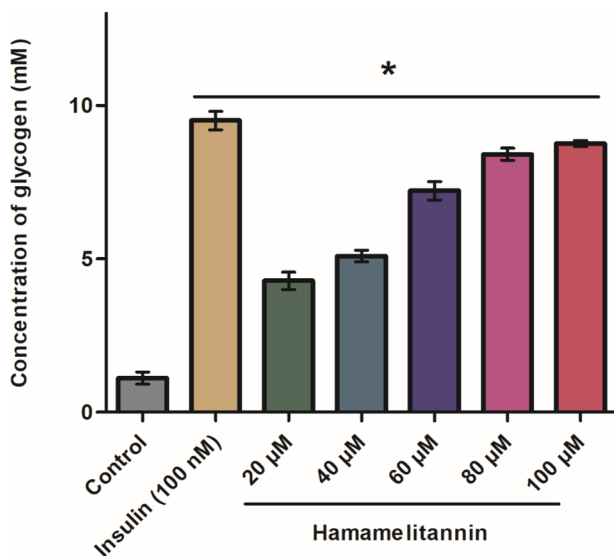


Fig. 4 Dose-response analysis of hamamelitannin (20 μM to 100 μM) in glycogen synthesis in L6 myotubes. The concentration of glycogen was measured on L6 myotubes at indicated doses of hamamelitannin at 24 h. 100 nM Insulin were used as positive control. The concentration of glycogen was expressed as mM. Data represent the mean \pm SD in three independent experiments in triplicates. * $p < 0.05$ as compared with control

GLUT-4 expression

The localization of GLUT 4 in the cell was studied using confocal microscopy. L6 myotubes were deprived of serum and treated with an optimum concentration of 100 μM hamamelitannin for 24 h compared to the untreated control cells. Hamamelitannin (100 μM) treatment enhanced the GLUT-4 expression within the L6 myotubes cell (Fig. 7a and f).

Hamamelitannin on GLUT-4 nuclear translocation

The PM fractions were isolated using density gradient centrifugation and further subjected to immunoblot (Fig. 8a). Results revealed that hamamelitannin exposure had significantly ($p < 0.05$) increased the GLUT-4 protein content in PM fractions at 24 h. Expression levels were quantified by densitometry method (Fig. 8b). Hamamelitannin (100 μM) and insulin showed 2.6- and 2.8-fold increase in GLUT-4 expression levels, respectively in the PM fraction.

Discussion

Diabetes, a chronic disease which necessitates drug therapy, is increasing in an epidemic proportion. Plants have been the primary source of drugs and bioactive compounds, and myriad drugs which are currently available, are either directly or indirectly, derived from them [42].

Mechanism of action of the plant compounds in diabetic treatment has proposed numerous possibilities in which they could be responsible for the anti-hyperglycemic and anti-hyperlipidemic effects. Some of them evidence their effects on pancreatic β cell activity (synthesis, release, cell regeneration/revitalization), enhancement in activity pertaining to its protective nature and increment of sensitivity of the hormone insulin or insulin-like activity of the plant compounds. Mechanisms which are involved in maintenance of stable glucose level in the body include amelioration of glycogenolysis by regulating enzymes, suppression of glucose absorption by intestinal cells and slack in glycogenic index of carbohydrates or reduction of the effect of glutathione [43]. The present investigation emphasises the defensive impact of hamamelitannin in L6 myotubes.

Skeletal muscle is one of the most important insulin-target tissues liable for repairs of regulation of blood sugar. Insulin stimulus of glucose uptake in skeletal muscle cells is facilitated through translocation of GLUT-4 from the endoplasmic reticulum to the PM [44]. Skeletal muscle is a suitable model for the study of glucose transportation. Skeletal muscles are the major site for glucose utilization and disposal [45]. Rat skeletal muscle L6 myotubes cell line which were secluded primarily by rat thigh muscle which fuse upon culturing in medium form multinucleated myotubes and striated fibres that is suitable model for in vitro study. An earlier report on L6 myotubes demonstrated that troglitazone was able to enhance the glucose transport two fold over control [46].

MTT [3-(4,5-dimethylthiazol-2-yl)-2,5 diphenyl tetrazolium bromide] assay principled on the transformation of formazan crystals from MTT, corresponds to mitochondrial activity related to the number of viable cells [47]. As shown in Fig. 1, treatment of the cells with varying concentration of hamamelitannin from 20 to 100 μM did not alter the cell viability indicating that they were not cytotoxic even at the highest concentration tested.

Hamamelitannin were examined for 2-deoxy-D-[1- ^3H]-glucose uptake; this 2-deoxy-D-[1- ^3H]-glucose accumulates in the cell after its entry into the cells as it cannot be metabolized further and hence the up taken glucose can be exactly determined. Treatment of L6 myotubes with various concentrations of hamamelitannin (20 to 100 μM) were assessed for glucose uptake activity. A dose-dependant augment in glucose uptake was observed and prime concentration exhibit utmost activity for hamamelitannin was found to be 100 μM (Fig. 2). These results are suggestive of insulinomimetic activity of hamamelitannin as they bind to the target tissue (skeletal muscles), thereby stimulate the downstream signaling events such as IRTK and PI3K activation, which is quintessential importance in glucose uptake. Similar result was observed in Acacetin which enhanced

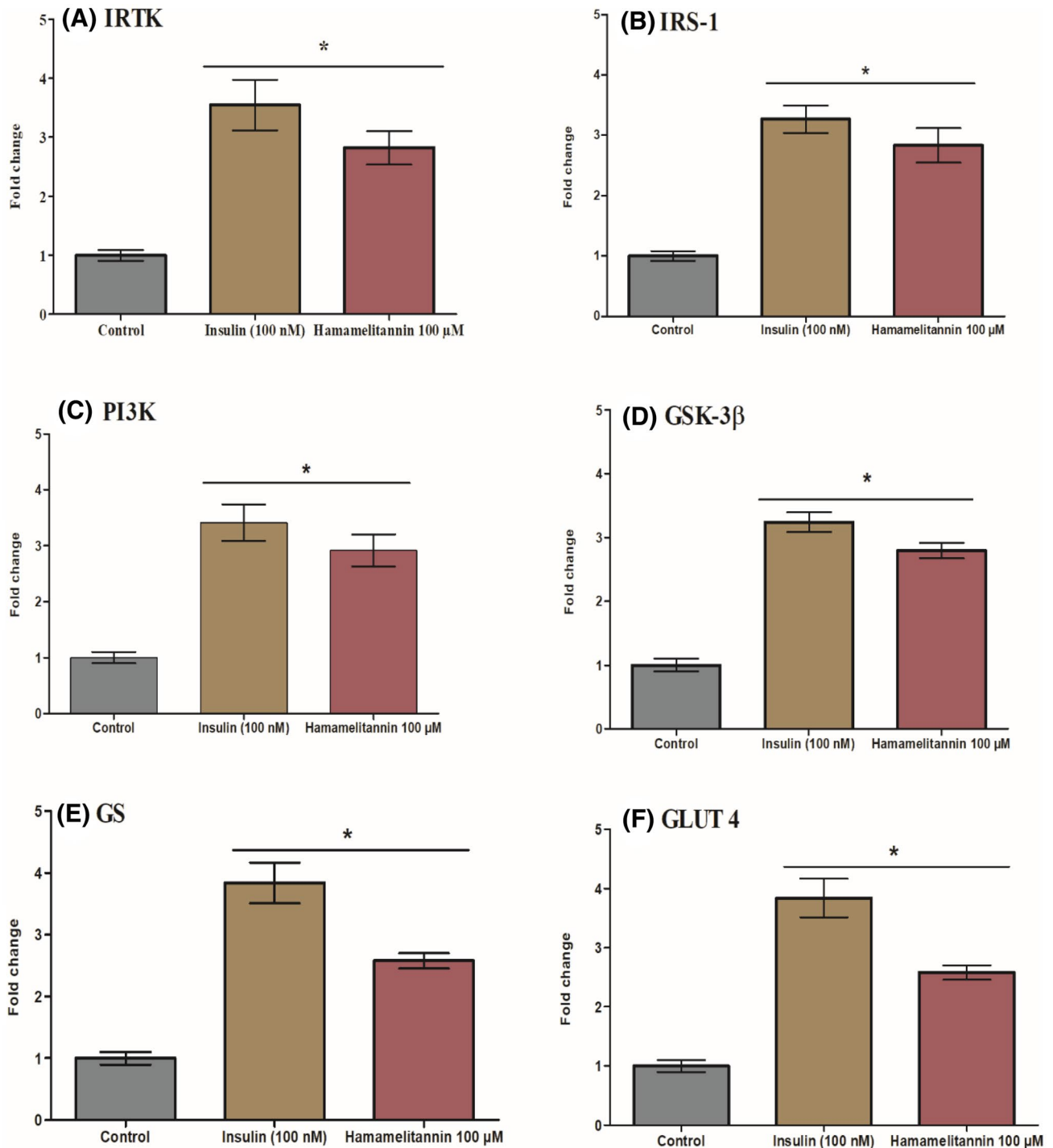


Fig. 5 a–f Effects of extracts on **a** IRTK, **b** IRS-1, **c** PI3K, **d** GSK-3 β , **e** GS and **f** GLUT-4 mRNA expression level using quantitative (real-time) PCR. 100 nM Insulin were used as positive control. The reactions were prepared according to the standard protocol for one

step KAPA SYBR[®] FAST qPCR Kit Master Mix (2 \times). Data were expressed as mean \pm SD of three independent experiments in triplicates. * p < 0.05 as compared with control

the glucose uptake through insulin-independent GLUT-4 translocation in L6 myotubes that strengthens our data [48].

Comparative analysis of glucose uptake in presence or absence of genistein, an IRTK inhibitor was carried

out. Genistein inhibits insulin-induced phosphorylation of the insulin receptor at the 4th and 8th tyrosine residues, thereby lowering the glucose uptake activity. The percentage glucose uptake was significantly lowered (p < 0.05)

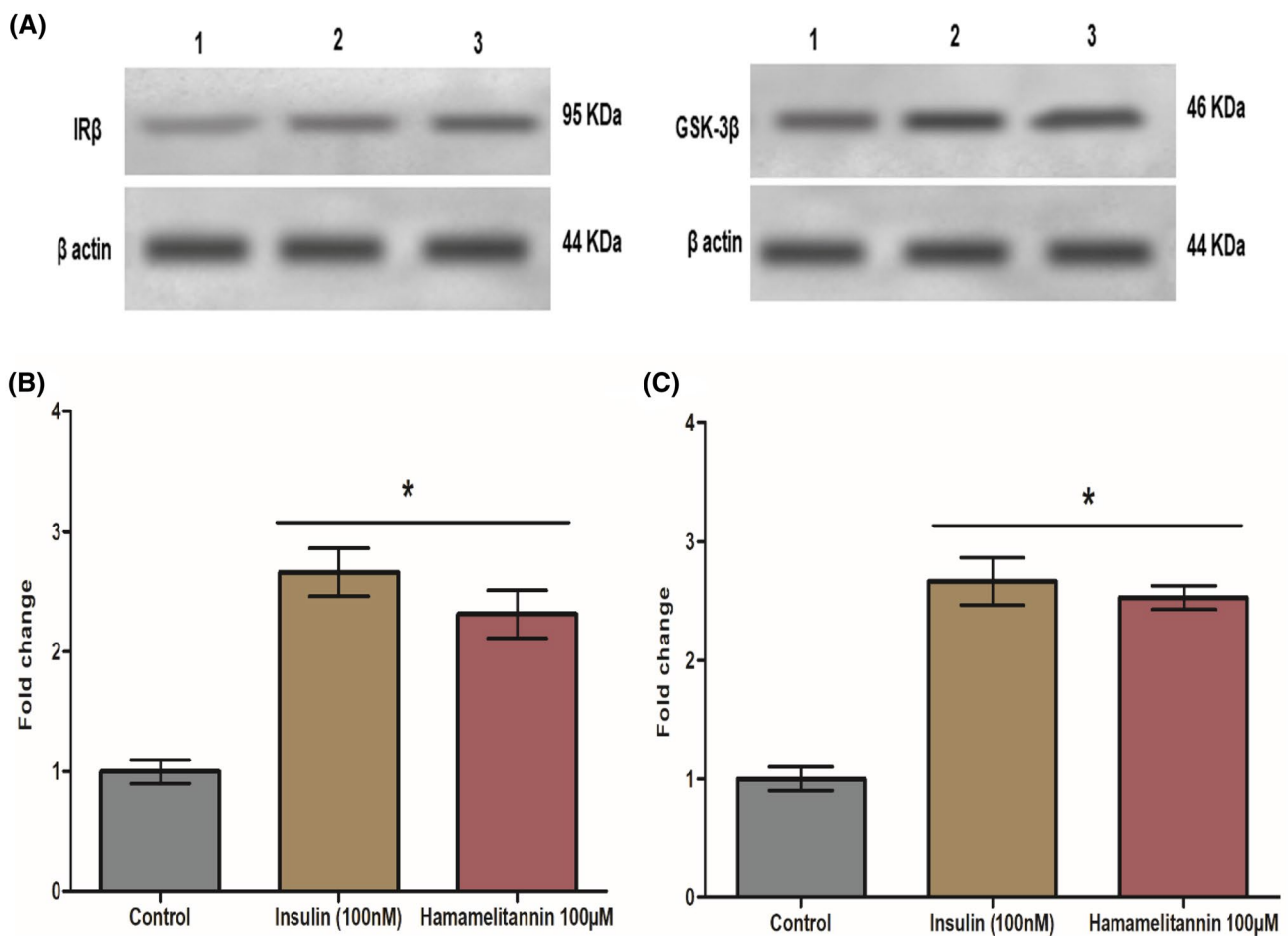


Fig. 6 a Effect of hamamelitannin on protein expression at 24 h. Lane 1 denotes untreated control, Lane 2 Insulin (100 nM) was used as positive control, and Lane 3 indicates hamamelitannin (100 μM) treated cells respectively. IRβ and GSK-3β protein expressions were

shown. β actin served as a loading control. IRβ (b) and GSK-3β (c) protein expression upon treatment with hamamelitannin (100 μM). Data were expressed as mean ± SD of three independent experiments in triplicates. * $p < 0.05$ as compared with control

in the presence of genistein for the cells treated with the hamamelitannin. This validated the claim that the hamamelitannin mediate glucose uptake through IRTK activation (Fig. 3a). Glucose uptake activation upon treatment with hamamelitannin was strongly inhibited by genistein suggesting that the transport of glucose is unquestionably reliant on activation of the insulin receptor.

Wortmannin is a selective inhibitor of PI3K [49]. Since the treated cells showed a decrease in glucose uptake with wortmannin ($96.7 \pm 2.1\%$), the glucose uptake activity was observed in hamamelitannin pre-treated with wortmannin as compared with the treated cells in the absence of inhibitor which showed $200.2 \pm 2.6\%$ of glucose uptake (Fig. 3b). The results revealed that hamamelitannin mimic insulin by reverting insulin resistance through PI3K activation. Therefore, it can be inferred the glucose uptake which is mediated through IRTK and PI3K dependent pathway.

Earlier report [33] have shown that in existence of Genistein and Wortmannin inhibitors (3β)-stigmast-5-en-3-ol pretreatment with genistein resulted in glucose uptake reduction from 67.20 ± 7 to $49.68 \pm 3\%$; and wortmannin show decline in glucose uptake from 50.67 ± 3 to $41.35 \pm 6\%$, it suggests the contribution of IRTK and PI3K in boosting transport of glucose. Our results provide the evidence that hamamelitannin enhances the glucose transport through activation of IRTK and PI3K.

Insulin increases glucose utilization in the muscle by stimulating transport of glucose and initiating glycogen synthase enzyme for the synthesis of glycogen. The deactivated glycogen synthase is impaired in skeletal muscle of diabetics with glucose intolerance and insulin resistance [50]. In addition to the play of insulin in synthesis of glycogen, PKB showed a significant role in insulin facilitating glucose transportation and glycogen synthesis [51]. The stimulated

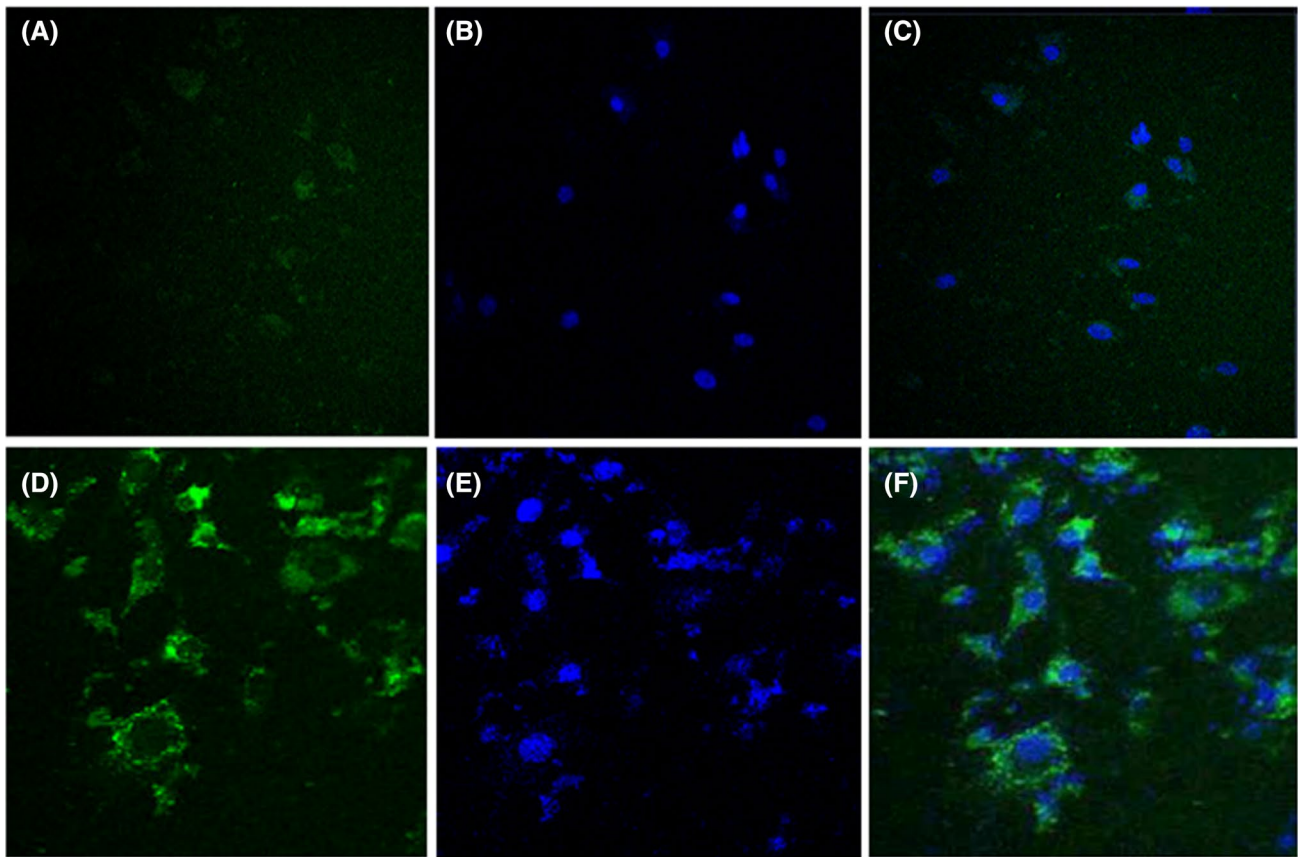


Fig. 7 Confocal microscopic analysis using FITC tagged GLUT-4 in L6 myotubes. **a–c** Refer to untreated control cells, **a** refers to the fluorescence pattern with FITC (543 nm) and **b** with DAPI stain (461 nm) and **c** refers to merged images of FITC and DAPI. **d** refers

to hamamelitannin (100 μ M) treated cells, the fluorescence pattern of the cells emitted at 543 nm (FITC). **e** Refers to the hamamelitannin (100 μ M) treated cells with DAPI stain (emission at 461 nm). **f** Refers to the merged images of FITC and DAPI

PKB upsurges GS over an inhibition of GSK3- β [52, 53] because the active GSK3- β is the key donor of insulin resistance. Grounded on this the hamamelitannin was examined for its role in synthesis of glycogen in L6 myotubes and the optimum concentration of hamamelitannin was found to be 100 μ M which enabled the synthesis of 8.7 mM of glycogen in L6 myotubes (Fig. 4). Hamamelitannin promoted glucose storage by activating PKB and inhibiting GSK3- β , thus aiding glycogen synthesis. Similarly, Aloe emodin glycosides isolated from *Cassia fistula* stimulates the uptake of glucose and storage of glycogen via insulin signaling pathway, hence exhibiting a significant increase in glycogen synthesis 121% at 100 μ g/mL [54].

To examine the molecular-mechanisms beneath the effects of hamamelitannin on glucose uptake, IRTK, IRS-1, PI3K, GLUT-4, GSK-3 β and GS mRNA expression was quantified using Real Time-PCR. The results revealed that hamamelitannin treated cells significantly increased the expression of IRTK, IRS-, PI3K, GLUT-4, GSK-3 β and GS (Fig. 5a–f). These results propound that hamamelitannin trigger insulin to bind to its tyrosine kinase receptor,

leading to tyrosine phosphorylation of insulin receptor substrate (IRS-1), followed by the activation of PI3K. The downstream targets of PI3K includes AKT/PKB (Protein Kinase B) and PKC, whose activation/phosphorylation triggers the translocation of GLUT-4 to the plasma membrane and increases glycogen synthase through inhibition of GSK-3 β . Previous study [55] demonstrated that tannins present in *Cichorium intybus* enhanced GLUT-4 and PI3K mRNA expression. Sujatha et al. [33] reported that crude as well as (3 β)-STIGMAST-5-EN-3-OL were capable to extensively augment mRNA expression of IRTK, IRS-1 and PI3K followed by downstream kinases activation. Cinnamaldehyde at altered concentrations such as 10, 20 and 50 μ M in C2C12 cell line increased GLUT 4 gene expression by 1.25, 1.6 and 3.01 folds, correspondingly when compared with the control cells [56].

Insulin binds to IR prompting the downstream signaling events leading to a betterment in glucose uptake. Diabetic patients linked with lessen level of IR β have been reported [57]. Optimum concentration of hamamelitannin (100 μ M) remarkably enhanced the phosphorylation of key insulin

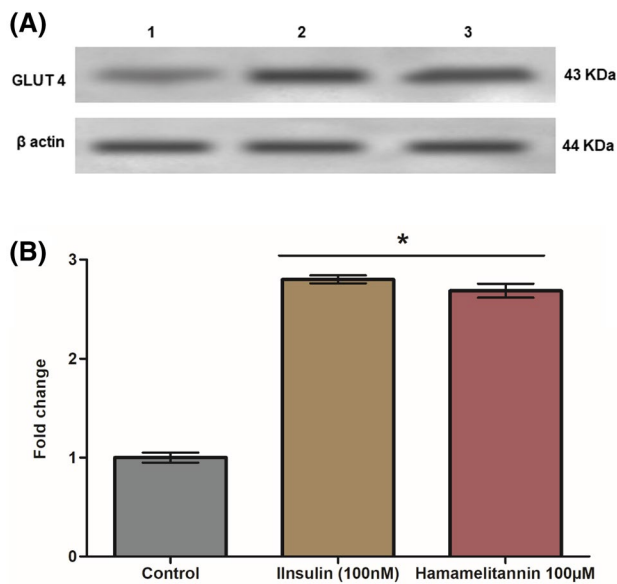


Fig. 8 **a** Protein expression of GLUT-4 by hamamelitannin (100 μ M) at 24 h. 100 nM Insulin was used as a positive control. Lane 1 denotes untreated control, Lane 2 Insulin (100 nM), Lane 3 indicates hamamelitannin (100 μ M). **b** Densitometric analysis of translocation of GLUT-4 using PM fractions. The fold increase of GLUT-4 upon treatment with hamamelitannin was quantified arbitrarily. The data was expressed over untreated control. Data were expressed as mean \pm S.D of three independent experiments in triplicates. * $p < 0.05$ as compared with control

signaling marker IR β , similar to positive control as shown in Fig. 6a and b. Reports have proven that triterpenoids [57], AEG [54], (3 β)-STIGMAST-5-EN-3-OL [33] can activate IR β and mimic insulin in exerting the anti-diabetic efficacy.

PKB has a quintessential task in insulin-mediated glucose transport and glycogen synthesis. PKB activation inhibits GSK-3 β and increase the glycogen synthesis [58]. Various reports have shown that GSK-3 β inhibitors promote an upshot in glycogen synthesis and insulin sensitivity. Instigation of GSK-3 β contributes to lesser synthesis of glycogen and decreased insulin sensitivity. The insulin sensitivity and glycogen metabolism support the role of GSK-3 β in the regulation of insulin action in skeletal muscle [59–61]. The optimum concentration of hamamelitannin showed increase in GSK-3 β (serine phosphorylation at 9th residue) in L6 myotubes thereby suggesting the inactivation of GSK-3 β as shown in Fig. 6a, c. These results evince that hamamelitannin follow the footsteps of insulin in activating GSK-3 β and contributing to its insulinomimetic activity. Anand et al. [54] have proved that AEG prompt glucose storage through the inhibition of pGSK-3 β and activation of PKB.

The next important target is GLUT-4 as it is a major glucose transporter in skeletal muscles. Impairment in this translocation is the major cause of insulin resistance, it is therefore important to actuate GLUT-4 in skeletal muscle to

ease insulin resistance. The localization of GLUT-4 in the cell was studied using confocal microscopy. Hamamelitannin exhibited enhanced fluorescence within the cell which proves the localization of GLUT-4 inside the cell (Fig. 7). Similar results were observed with (3 β)-STIGMAST-5-EN-3-OL, which showed increased fluorescence throughout the cell, thereby suggesting the increased GLUT-4 content within the cell prior to the translocation [33]. The increase in glucose uptake by hamamelitannin is attributable to the translocation of GLUT-4 from light microsomes to PM. This translocation pattern was studied semi-quantitatively by measuring the GLUT-4 protein content using immunoblot. Hamamelitannin (100 μ M) significantly increased the GLUT-4 protein content in PM fractions at 24 h (Fig. 8a and b). Previous study [22] with troglitazone revealed that the translocation of GLUT-4 from light microsome to the PM attributed to its glucose uptake efficacy, which supports our data.

Conclusions

In conclusion, the above studies in vitro, evidenced the anti-diabetic efficacy of hamamelitannin. The insulinomimetic activity evinced by hamamelitannin can be a key player in reverting insulin resistance and enhancing the synthesis of glycogen. Hamamelitannin treatment mediates the effect on glucose transport and metabolism in a IRTK and PI3K-dependent manner. Hamamelitannin exposure was also shown to upregulate the expression of key genes: IRS-1, GLUT-4 and GSK-3 β which involved in glucose transport machinery. Therefore, our findings suggest that hamamelitannin, thus could have a therapeutic value for the treatment against insulin resistance.

Acknowledgements The authors extend their appreciation to The Researchers Supporting Project (RSP-2020/20), King Saud University, Riyadh, Saudi Arabia. Universiti Putra Malaysia contribution to the research is made possible through research grant LRGS/1/2019/UPM/1.

Compliance with ethical standards

Conflict of interest All authors declare that they have no conflict of interest.

Ethical approval This article does not contain any studies with human participants or animals performed by any of the authors.

References

1. Kamaraj N, Rajaguru PY, Issac P, kumar, Sundaresan S (2017) Fabrication, characterization, in vitro drug release and glucose uptake activity of 14-deoxy, 11, 12-didehydroandrographolide

- loaded polycaprolactone nanoparticles. *Asian J Pharm Sci* 12:353–362. <https://doi.org/10.1016/j.ajps.2017.02.003>
2. Praveen Kumar I, Arun J, Sri Sneha C, Sujatha S (2018) Tannins of *Jatropha gossypifolia* exert anti-hyperlipidemic effect. *Eur Biomed Pharm Sci* 5:607–614
 3. Zhu J, Chen Z, Zhou H, Yu C, Han Z, Shao S, Hu X, Wei X, Wang Y (2020) Effects of extraction methods on physicochemical properties and hypoglycemic activities of polysaccharides from coarse green tea. *Glycoconj J* 37:241–250. <https://doi.org/10.1007/s10719-019-09901-2>
 4. American Diabetes Association (2010) Diagnosis and classification of diabetes mellitus. *Diabetes Care* 33(Suppl 1):S62–S69. <https://doi.org/10.2337/dc10-S062>
 5. DeFronzo RA, Ferrannini E, Alberti KGMM, (Kurt GMM, Zimet P (2015) International textbook of diabetes mellitus. Wiley, New York
 6. Praveen Kumar I, Isha M, Sujatha S, Alwin D: Antihyperglycemic and antihyperlipidemic activity of *Jatropha gossypifolia* methanolic extract in streptozotocin-nicotinamide induced diabetic rats. *Asian J Pharm Clin Res* 10, 326–330 (2017). <https://doi.org/10.22159/ajpcr.2017.v10i11.20985>
 7. Reaven G (2004) The metabolic syndrome or the insulin resistance syndrome? Different names, different concepts, and different goals. *Endocrinol Metab Clin N Am* 33:283–303. <https://doi.org/10.1016/j.ecl.2004.03.002>
 8. Jayakumar A, Gardner DG, Shoback D (2012) Greenspan's basic and clinical endocrinology. Yale J Biol Med 85:559
 9. Wheatcroft SB, Williams IL, Shah AM, Kearney MT (2003) Pathophysiological implications of insulin resistance on vascular endothelial function. *Diabet Med* 20:255–268
 10. Smith U (2002) Impaired ('diabetic') insulin signaling and action occur in fat cells long before glucose intolerance—is insulin resistance initiated in the adipose tissue? *Int J Obes Relat Metab Disord* 26:897–904. <https://doi.org/10.1038/sj.ijo.0802028>
 11. Giorgino F, Laviola L, Eriksson JW (2005) Regional differences of insulin action in adipose tissue: insights from in vivo and in vitro studies. *Acta Physiol Scand* 183:13–30. <https://doi.org/10.1111/j.1365-201X.2004.01385.x>
 12. Hunter SJ, Garvey WT (1998) Insulin action and insulin resistance: diseases involving defects in insulin receptors, signal transduction, and the glucose transport effector system. *Am J Med* 105:331–345
 13. Academic H, GmbH P, Sakurai H (1995) Peroxyl radical scavenging activities of hamamelitannin in chemical and biological systems. *Free Radic Res* 22:419–430
 14. Habtemariam S (2002) Hamamelitannin from *Hamamelis virginiana* inhibits the tumour necrosis factor- α (TNF)-induced endothelial cell death in vitro. *Toxicol* 40:83–88
 15. Kiran MD, Adikesavan NV, Cirioni O, Giacometti A, Silvestri C, Scalise G, Ghiselli R, Saba V, Orlando F, Shoham M, Balaban N (2008) Discovery of a quorum-sensing inhibitor of drug-resistant staphylococcal infections by structure-based virtual screening. *Mol Pharmacol* 73:1578–1586. <https://doi.org/10.1124/mol.107.044164.devices>
 16. Sánchez-Tena S, Fernández-Cachón ML, Carreras A, Mateos-Martín ML, Costoya N, Moyer MP, Nuñez MJ, Torres JL (2012) Hamamelitannin from witch hazel (*Hamamelis virginiana*) displays specific cytotoxic activity against colon cancer cells. *J Nat Prod* 75:26–33. <https://doi.org/10.1021/np200426k>
 17. Cobrado L, Azevedo MM, Ramos JP, Rodrigues AG (2012) Cerium, chitosan and hamamelitannin as novel biofilm inhibitors? *J Antimicrob Chemother* 8:2–5. <https://doi.org/10.1093/jac/dks007>
 18. Anandharajan R, Jaiganesh S, Shankernarayanan NP, Viswakarma RA, Balakrishnan A (2006) In vitro glucose uptake activity of *Aegles marmelos* and *Syzygium cumini* by activation of Glut-4, PI3 kinase and PPAR γ in L6 myotubes. *Phytomedicine* 13:434–441. <https://doi.org/10.1016/j.phymed.2005.03.008>
 19. Walgren JLE, Vincent TS, Schey KL, Buse MG (2003) High glucose and insulin promote O-GlcNAc modification of proteins, including α -tubulin. *Am J Physiol Endocrinol Metab* 284(2):E424–E434
 20. Mosmann T (1983) Rapid colorimetric assay for cellular growth and survival: application to proliferation and cytotoxicity assays. *J Immunol Methods* 65:55–63. [https://doi.org/10.1016/0022-1759\(83\)90303-4](https://doi.org/10.1016/0022-1759(83)90303-4)
 21. Yonemitsu S, Nishimura H, Shintani M, Inoue R, Yamamoto Y, Masuzaki H, Ogawa Y, Hosoda K, Inoue G, Hayashi T, Nakao K (2001) Troglitazone induces GLUT4 translocation in L6 myotubes. *Diabetes* 50:1093–1101
 22. Parry HA, Rivera ME, Vaughan RA, Sunderland KL (2020) Uncarboxylated osteocalcin decreases insulin-stimulated glucose uptake without affecting insulin signaling and regulators of mitochondrial biogenesis in myotubes. *J Physiol Biochem*. <https://doi.org/10.1007/s13105-020-00732-6>
 23. Bazuine M, van den Broek PJA, Maassen JA (2005) Genistein directly inhibits GLUT4-mediated glucose uptake in 3T3-L1 adipocytes. *Biochem Biophys Res Commun* 326:511–514. <https://doi.org/10.1016/j.bbrc.2004.11.055>
 24. Roe JH, Dailey RE (1966) Determination of glycogen with the anthrone reagent. *Anal Biochem* 15:245–250. [https://doi.org/10.1016/0003-2697\(66\)90028-5](https://doi.org/10.1016/0003-2697(66)90028-5)
 25. Fisher Scientific - TRIZOL: TRIZOL Reagent User Guide - Pub. No. MAN0001271 - Rev. A.0. 15596018
 26. Arockiaraj J, Easwaran S, Vanaraja P, Singh A, Othman RY, Bhassu S (2012) Prophenoloxidase activating enzyme-III from giant freshwater prawn *Macrobrachium rosenbergii*: characterization, expression and specific enzyme activity. *Mol Biol Rep* 39:1377–1386. <https://doi.org/10.1007/s11033-011-0872-5>
 27. Kumaresan V, Bhatt P, Palanisamy R, Gnanam AJ, Pasupuleti M, Arockiaraj J (2014) A murrel cysteine protease, cathepsin L: bioinformatics characterization, gene expression and proteolytic activity. *Biologia* 69:395–406. <https://doi.org/10.2478/s11756-013-0326-8>
 28. Arockiaraj J, Vanaraja P, Easwaran S, Singh A, Alinejad T, Othman RY, Bhassu S (2011) Gene profiling and characterization of arginine kinase-1 (MrAK-1) from freshwater giant prawn (*Macrobrachium rosenbergii*). *Fish Shellfish Immunol* 31:81–89. <https://doi.org/10.1016/j.fsi.2011.04.004>
 29. Chomczynski P, Sacchi N (1987) Single-step method of RNA isolation by acid guanidinium thiocyanate-phenol-chloroform extraction. *Anal Biochem* 162:156–159. [https://doi.org/10.1016/0003-2697\(87\)90021-2](https://doi.org/10.1016/0003-2697(87)90021-2)
 30. Arockiaraj J, Easwaran S, Vanaraja P, Singh A, Othman RY, Bhassu S (2012) Molecular cloning, characterization and gene expression of an antioxidant enzyme catalase (MrCat) from *Macrobrachium rosenbergii*. *Fish Shellfish Immunol* 32:670–682. <https://doi.org/10.1016/j.fsi.2012.01.013>
 31. Arockiaraj J, Gnanam AJ, Muthukrishnan D, Thirumalai MK, Pasupuleti M, Milton J, Kasi M (2013) *Macrobrachium rosenbergii* cathepsin L: Molecular characterization and gene expression in response to viral and bacterial infections. *Microbiol Res* 168:569–579. <https://doi.org/10.1016/j.micres.2013.04.007>
 32. Chaurasia MK, Nizam F, Ravichandran G, Arasu MV, Al-Dhabi NA, Arshad A, Elumalai P, Arockiaraj J (2016) Molecular importance of prawn large heat shock proteins 60, 70 and 90. *Fish Shellfish Immunol* 48:228–238. <https://doi.org/10.1016/j.fsi.2015.11.034>
 33. Sujatha S, Anand S, Sangeetha KN, Shilpa K, Lakshmi J, Balakrishnan A, Lakshmi BS (2010) Biological evaluation of (3 β)-STIGMAST-5-EN-3-OL as potent anti-diabetic agent in

- regulating glucose transport using in vitro model. *Int J Diabetes Mellitus* 2:101–109. <https://doi.org/10.1016/j.ijdm.2009.12.013>
34. Bhatt P, Kumaresan V, Palanisamy R, Chaurasia MK, Gnanam AJ, Pasupuleti M, Arockiaraj J (2014) Immunological role of C4 CC chemokine-1 from snakehead murrel *Channa striatus*. *Mol Immunol* 57:292–301. <https://doi.org/10.1016/j.molimm.2013.10.012>
 35. Kumaresan V, Bhatt P, Ganesh MR, Harikrishnan R, Arasu MV, Al-Dhabi NA, Pasupuleti M, Marimuthu K, Arockiaraj J (2015) A novel antimicrobial peptide derived from fish goose type lysozyme disrupts the membrane of *Salmonella enterica*. *Mol Immunol* 68:421–433. <https://doi.org/10.1016/j.molimm.2015.10.001>
 36. Laville M, Auboeuf D, Khalfallah Y, Vega N, Riou JP, Vidal H (1996) Acute regulation by insulin of phosphatidylinositol-3-kinase, Rad, Glut 4, and lipoprotein lipase mRNA levels in human muscle. *J Clin Invest* 98:43–49. <https://doi.org/10.1172/JCI118775>
 37. Buhl ES, Jessen N, Schmitz O, Pedersen SB, Pedersen O, Holman GD, Lund S (2001) Chronic treatment with 5-aminoimidazole-4-carboxamide-1-beta-D-ribofuranoside increases insulin-stimulated glucose uptake and GLUT4 translocation in rat skeletal muscles in a fiber type-specific manner. *Diabetes* 50:12–17. <https://doi.org/10.2337/diabetes.50.1.12>
 38. Woodgett JR (1990) Molecular cloning and expression of glycogen synthase kinase-3/factor A. *EMBO J* 9:2431–2438
 39. Magnoni LJ, Vraskou Y, Palstra AP, Planas JV, McClelland G (2012) AMP-activated protein kinase plays an important evolutionary conserved role in the regulation of glucose metabolism in fish skeletal muscle cells. *PLoS ONE* 7:e31219. <https://doi.org/10.1371/journal.pone.0031219>
 40. Sahni SK, Turpin LC, Brown TL, Sporn LA (1999) Involvement of protein kinase C in *Rickettsia rickettsii*-induced transcriptional activation of the host endothelial cell. *Infect Immun* 67:6418–6423
 41. Kanaujia A, Duggar R, Pannakal ST, Yadav SS, Katiyar CK, Bansal V, Anand S, Sujatha S, Lakshmi BS (2010) Insulinomimetic activity of two new gallotannins from the fruits of *Capriparis moonii*. *Bioorg Med Chem* 18:3940–3945. <https://doi.org/10.1016/j.bmc.2010.04.032>
 42. Priyanka, Singh R (2016) A systematic review on indian floral biodiversity as eminent reserves for alternative treatment strategy of diabetes mellitus. *Int J Pharm Pharm Sci* 8:10–19
 43. Sharma PK, Srivastava P, Kumar N, Dudhe R (2010) Plants having potential antidiabetic activity: a review. *Der Pharm Lett* 2:369–387
 44. Ishiki M, Klip A (2005) Minireview: recent developments in the regulation of glucose transporter-4 traffic: new signals, locations, and partners. *Endocrinology* 146:5071–5078. <https://doi.org/10.1210/en.2005-0850>
 45. Koivisto UM, Martinez-Valdez H, Bilan PJ, Burdett E, Ramlal T, Klip A (1991) Differential regulation of the GLUT-1 and GLUT-4 glucose transport systems by glucose and insulin in L6 muscle cells in culture. *J Biol Chem* 266:2615–2621
 46. Ciaraldi TP, Huber-Knudsen K, Hickman M, Olefsky JM (1995) Regulation of glucose transport in cultured muscle cells by novel hypoglycemic agents. *Metabolism* 44:976–981
 47. van Meerloo J, Kaspers GJL, Cloos J (2011) Cell sensitivity assays: the MTT assay. *Methods Mol Biol* 731:237–245
 48. Kwon E, Bin, Kang MJ, Ryu HW, Lee S, Lee JW, Lee MK, Lee HS, Lee SU, Oh SR, Kim MO (2020) Acacetin enhances glucose uptake through insulin-independent GLUT4 translocation in L6 myotubes. *Phytomedicine* 68:153178. <https://doi.org/10.1016/j.phymed.2020.153178>
 49. Luca JP, De Garnache AK, Rulf J, Miller TB, Laviola L, Bel-santi G, Davalli AM, Napoli R, Perrini S, Gordon C, Giorgino R, Giorgino F, Luca D, Jane P (2011) Wortmannin inhibits insulin-stimulated activation of protein phosphatase 1 in rat cardiomyocytes. *Am J Physiol* 276(5):1520–1526
 50. Nikoulina SE, Ciaraldi TP, Carter L, Mudaliar S, Park KS, Henry RR (2011) Impaired muscle glycogen synthase in type 2 diabetes is associated with diminished phosphatidylinositol 3-kinase activation. *J Clin Endocrinol Metab* 86(9):4307–4314
 51. Jiang ZY, Zhou QL, Coleman KA, Chouinard M, Boese Q, Czech MP (2003) Insulin signaling through Akt/protein kinase B analyzed by small interfering RNA-mediated gene silencing. *Proc Natl Acad Sci USA* 100:7569–74. <https://doi.org/10.1073/pnas.1332633100>
 52. MacAulay K, Blair AS, Hajdich E, Terashima T, Baba O, Sutherland C, Hundal HS (2005) Constitutive activation of GSK3 down-regulates glycogen synthase abundance and glycogen deposition in rat skeletal muscle cells. *J Biol Chem* 280:9509–9518. <https://doi.org/10.1074/jbc.M411648200>
 53. Cross DA, Alessi DR, Cohen P, Andjelkovich M, Hemmings BA (1995) Inhibition of glycogen synthase kinase-3 by insulin mediated by protein kinase B. *Nature* 378:785–789. <https://doi.org/10.1038/378785a0>
 54. Anand S, Muthusamy VS, Sujatha S, Sangeetha KN, Raja B, Sudhagar R, Poornima Devi S, Lakshmi N (2010) B.S.: Aloe emodin glycosides stimulates glucose transport and glycogen storage through PI3K dependent mechanism in L6 myotubes and inhibits adipocyte differentiation in 3T3L1 adipocytes. *FEBS Lett* 584:3170–3178. <https://doi.org/10.1016/j.febslet.2010.06.004>
 55. Muthusamy VS, Anand S, Sangeetha KN, Sujatha S, Arun B, Lakshmi BS (2008) Tannins present in *Cichorium intybus* enhance glucose uptake and inhibit adipogenesis in 3T3-L1 adipocytes through PTP1B inhibition. *Chem Biol Interact* 174:69–78. <https://doi.org/10.1016/j.cbi.2008.04.016>
 56. Nikzamir A, Palangi A, Kheirollaha A, Tabar H, Malakaskar A, Shahbazian H, Fathi M (2014) Expression of glucose transporter 4 (GLUT4) is increased by cinnamaldehyde in C2C12 mouse muscle cells. *Iran Red Crescent Med J* 16:e13426. <https://doi.org/10.5812/ircmj.13426>
 57. Goodyear LJ, Giorgino F, Sherman LA, Carey J, Smith RJ, Dohm GL (1995) Insulin receptor phosphorylation, insulin receptor substrate-1 phosphorylation, and phosphatidylinositol 3-kinase activity are decreased in intact skeletal muscle strips from obese subjects. *J Clin Invest* 95:2195–2204. <https://doi.org/10.1172/JCI117909>
 58. Cross DA, Alessi DR, Vandenhede JR, McDowell HE, Hundal HS, Cohen P (1994) The inhibition of glycogen synthase kinase-3 by insulin or insulin-like growth factor 1 in the rat skeletal muscle cell line L6 is blocked by wortmannin, but not by rapamycin: evidence that wortmannin blocks activation of the mitogen-activated protein kin. *Biochem J* 303(Pt 1):21–26
 59. Ilouz R, Kowalsman N, Eisenstein M, Eldar-Finkelman H (2006) Identification of novel glycogen synthase kinase-3 β substrate-interacting residues suggests a common mechanism for substrate recognition. *J Biol Chem* 281:30621–30630. <https://doi.org/10.1074/jbc.M604633200>
 60. Liberman Z, Eldar-Finkelman H (2005) Serine 332 phosphorylation of insulin receptor substrate-1 by glycogen synthase kinase-3 attenuates insulin signaling. *J Biol Chem* 280:4422–4428. <https://doi.org/10.1074/jbc.M410610200>
 61. Henriksen EJ, Kinnick TR, Teachey MK, O'Keefe MP, Ring D, Johnson KW, Harrison SD (2003) Modulation of muscle insulin resistance by selective inhibition of GSK-3 in Zucker diabetic fatty rats. *Am J Physiol Endocrinol Metab* 284:E892–E900. <https://doi.org/10.1152/ajpendo.00346.2002>

Affiliations

Praveen Kumar Issac¹  · Ajay Guru¹  · Sri Snehaa Chandrakumar²  · Christy Lite³  · N. T. Saraswathi⁴  · Mariadhas Valan Arasu⁵  · Naif Abdullah Al-Dhabi⁵  · Aziz Arshad^{6,7}  · Jesu Arockiaraj¹ 

Praveen Kumar Issac
praveenkumarissac@gmail.com

Ajay Guru
ajayrag02@gmail.com

Sri Snehaa Chandrakumar
snehaa.zeus@gmail.com

Christy Lite
christylite8@gmail.com

N. T. Saraswathi
saras@scbt.sastra.edu

Mariadhas Valan Arasu
mvalanarasu@gmail.com

Naif Abdullah Al-Dhabi
naifaldhabi2014@gmail.com

Aziz Arshad
azizar.upm@gmail.com

² Department of Biotechnology, Anna University, BIT Campus, Tiruchirappalli, Tamil Nadu 620 024, India

³ Endocrine and Exposome Laboratory, Department of Zoology, Madras Christian College, Tambaram, Chennai, Tamil Nadu 600 059, India

⁴ Molecular Biophysics Laboratory, School of Chemical and Biotechnology, SASTRA Deemed to be University, Thanjavur, Tamil Nadu 613 401, India

⁵ Department of Botany and Microbiology, College of Science, King Saud University, P.O. Box 2455, 11451 Riyadh, Saudi Arabia

⁶ International Institute of Aquaculture and Aquatic Sciences (I-AQUAS), Universiti Putra Malaysia, Port Dickson, Negeri Sembilan 71050, Malaysia

⁷ Department of Aquaculture, Faculty of Agriculture, Universiti Putra Malaysia, Serdang, Selangor 43400, Malaysia

¹ SRM Research Institute, SRM Institute of Science and Technology, Kattankulathur, Chennai, Tamil Nadu 603 203, India